

Topological rf -SQUID with a frustrating π -junction for probing the Majorana Bound State

P. Lucignano^{1,2}, F. Tafuri^{3,1}, and A. Tagliacozzo^{2,1}

¹ CNR-SPIN, Monte S. Angelo – via Cinthia, I-80126 Napoli, Italy

² Dipartimento di Scienze Fisiche, Università di Napoli “Federico II”, Monte S. Angelo, I-80126 Napoli, Italy and

³ Dipartimento Ingegneria dell’Informazione, Seconda Università di Napoli, I-81031 Aversa (CE), Italy

(Dated: February 22, 2013)

Majorana Bound States are predicted to appear as boundary states of the Kitaev model. Here we show that a π -Josephson Junction, inserted in a topologically non trivial model ring, sustains a Majorana Bound State, which is robust with respect to local and non local perturbations. The realistic structure could be based on a High Tc Superconductor tricrystal structure, similar to the one used to spot the d-wave order parameter. The presence of the Majorana Bound State changes the ground state of the topologically non trivial ring in a measurable way, with respect to that of a conventional one.

After the pioneering theoretical proposal by Kitaev[1], Majorana Fermions (MFs) have been predicted in a wide class of low-dimensional solid state devices. Being neutral excitations in Fractional Quantum Hall systems or hybrid superconducting devices, MFs are highly attractive for quantum computing gates, as well as for fundamental reasons. Despite the considerable theoretical and experimental efforts [2], challenges still remain before a real solid state device can be realized, allowing for isolation and manipulation of MFs. Among the promising engineered systems, there are quasi one-dimensional superconductors in contact with topological insulators (TIs) [3] or quasi one-dimensional systems with strong spin orbit interactions [4–7], helical magnets [8] and other materials [9–13]. However several issues have to be convincingly solved [14–16] and the recently announced experimental realizations [17–19] still arise excitement and debate [20].

Herewith we provide evidence that the richer functionalities of High Tc Superconductors (HTS), hybridized with topologically non trivial materials, can be used to monitor unambiguously the emergence of MFs in the ground state (GS) of a SQUID Josephson ring.

Epitaxial growths of high Tc cuprates, matching three differently orientated crystals, has provided in the past the evidence for the d -wave symmetry of the superconducting order parameter (OP) in HTS materials [21]. In Ref. [21] the experiment has been properly designed so that the ring contains an odd number of π -junctions and has a total critical current (I_c) and an inductance (L) to guarantee $I_c L \gg \phi_0$ (here $\phi_0 = hc/2e$ is the superconductive flux quantum). Its GS spontaneously breaks the time reversal symmetry with a current flowing in the ring and generating a spontaneous fractional flux $\phi = \pm\phi_0/2$ that can be measured by scanning SQUID microscopy [22].

The Kitaev model offers a very rich playground to study topological non trivial states. Inspired by the concept that any superconducting loop with an odd number of π junctions has a frustrated GS[23] (we call it “frustrated π -ring” ($F\pi R$) in the following), we study

a closed loop “Kitaev chain” [1], with a weak link having a jump of $\varphi = \pi$ in the phase of the OP (see Fig.1 for a sketch). Real life realizations of such a system could be a semiconducting wire with strong spin-orbit coupling (e.g. InAs or InSb), with spin polarizations splitted by a Zeeman magnetic field, or, alternatively, the edge state of a quasi two dimensional TI flake, such as Bi₂Se₃ or Bi₂Te₃. However, in this letter, we leave aside the details of the engineering of such devices and we focus on the model only. In particular we explicitly calculate the various branches in the energy dispersion of the Andreev Bound states $E_n(\varphi)$ of the model ring[1], finding a crossing of states of opposite fermionic parities \mathcal{P} at zero energy, which signals unambiguously the presence of the Majorana Bound State (MBS) in the spectrum.

As shown in Ref. [24], π junctions obtained by proximity induced superconductivity from nodal d-wave superconductors, can display a MBS at a phase difference $\varphi = 0$, rather than $\varphi = \pi$. Here we show that a corresponding state exists in the ring geometry depicted in Fig. 1 and is robust with respect to residual interactions, paving the way for an unambiguous measurement of its presence.

In general, the free energy describing a Josephson rf-SQUID ring shows minima at a phase difference φ which are directly related to a measurable spontaneous flux. In the conventional $F\pi R$ geometry, there is quite a high barrier separating the two minima at $\pm\phi_0/2$, which freezes the frustrated system in a time reversal symmetry broken GS. In our model, we find two minima close to $\pm\phi_0/2$ as well, as in the conventional $F\pi R$. However, they correspond to different parities. While the isolated model Hamiltonian conserves \mathcal{P} , this symmetry is rather unlikely to be maintained in the real life. In fact, impurities, trapping and releasing charges in the background, cannot be avoided. These events would correlate to flux quanta entering or leaving the ring, thus inducing tunneling of the system between the two minima, so that the expected average flux associated to the GS is $\langle\Phi\rangle = 0$. Measuring zero flux at a $F\pi R$ in presence of topologically

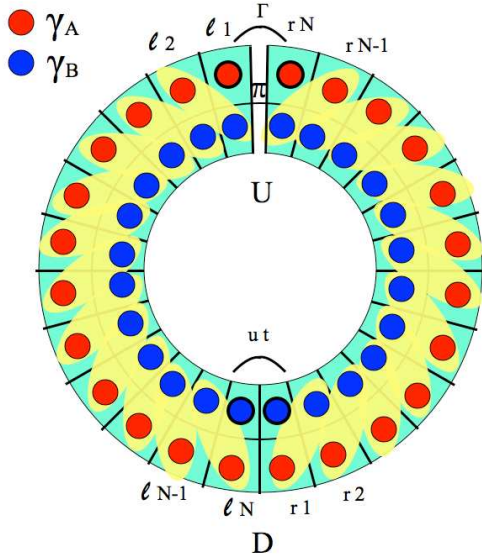


FIG. 1: (color online) Sketch of the Kitaev chain with a π -junction at the top point U . Red (blue) circles represent $\gamma_{A(B)}$ type MFs. Yellow ellipses signal strong coupling.

protected states would be the smoking gun evidence for the existence of the MBS in this device. It is a weird case that the breaking of the discrete symmetry (\mathcal{P}) enforces the time reversal symmetry to be restored.

Model Hamiltonian

We start considering a N -sites Kitaev chain of unitary lattice spacing and full length $L = 2N$, with real inter site hopping t . When folded in the shape of a ring the system displays mirror symmetry across the vertical line connecting points U and D between the top and the bottom (see Fig. 1).

Our device can be described as two N -sites Majorana wires (left (ℓ) and right (r)), coupled at the top of the ring U by the weak electron tunneling of energy Γ . At chemical potential $\mu = 0$, in the presence of an electromagnetic vector potential \vec{A} , the gauge invariant Hamiltonian reads as $H = H_\ell + H_r$, with:

$$H_\alpha = \sum_{j=1}^{N-1} \left(-\frac{t}{2} e^{ig_{\alpha j}} c_{\alpha j}^\dagger c_{\alpha j+1} + \frac{\Delta}{2} e^{i(\phi_{\alpha j} + \phi_{\alpha j+1})/2} c_{\alpha j} c_{\alpha j+1} + h.c. \right). \quad (1)$$

Here α labels the ℓ and r side of the ring, $c_{\alpha j}$ are spinless Dirac fermions at the site j and Δ is the superconducting pairing, generating an effective p-wave superconductivity. The phases $g_{\alpha j}$ acquired in the hopping between the j site and its nearest neighbor and the gauge invariant phase $\phi_{\alpha j}$ are defined as:

$$g_{\alpha j} = -\frac{e}{\hbar c} \int_{\alpha j}^{\alpha j+1} \vec{A} \cdot d\vec{l}, \quad (2)$$

$$\phi_{\alpha j} = \theta_{\alpha j} - \frac{2e}{\hbar c} \int_{\ell 1}^{\alpha j} \vec{A} \cdot d\vec{l}, \quad (3)$$

where $\theta_{\alpha j}$ is the phase of the superconducting order parameter.

At the top point U of the ring (see Fig.1) there is a tunnel junction which allows for the fractional Josephson coupling:

$$H_U = -\Gamma \left(c_{\ell 1}^\dagger c_{rN} + h.c. \right), \quad (4)$$

($\Gamma \ll t$). For sake of further investigations, we explicitly consider also the hopping term at the bottom point in the ring D , where the ℓ and r chains are matched:

$$H_D = -u t \left(c_{\ell N}^\dagger c_{r1} + h.c. \right). \quad (5)$$

Here we will keep the dimensionless parameter u (which may be complex) as a variable, to discuss also the limiting case of $u = 0$, which corresponds to the ring cut at D , with open ends.

The spinless Dirac fermions can be expressed in terms of two species of Majorana fermions at each site of the ring $\gamma_{A/Bj}^\alpha$, such that:

$$\gamma_{Bj}^\alpha = c_{\alpha j} e^{i\phi_{\alpha j}/2} + c_{\alpha j}^\dagger e^{-i\phi_{\alpha j}/2}, \quad (6)$$

$$\gamma_{Aj}^\alpha = -i \left(c_{\alpha j} e^{i\phi_{\alpha j}/2} - c_{\alpha j}^\dagger e^{-i\phi_{\alpha j}/2} \right). \quad (7)$$

A π -Josephson Junction requires Δ having opposite signs at U , between $\ell 1$ and rN . In the gauge in which Δ is real, the OP Δ has to vanish somewhere along the ring and we choose this point to be D with no loss of generality. As a first step, to make the approach as simplest as possible, deep in the topological phase, we will adopt the Kitaev approximation, $|\Delta| = t$ [1] all along the chain and we choose $\Delta = t$ in the ℓ region and $\Delta = -t$ in the r region of the ring. Thus, the chain Hamiltonian becomes:

$$H_\ell + H_r = -i \frac{t}{2} \sum_{j=1}^{N-1} [\gamma_{Bj}^\ell \gamma_{Aj+1}^\ell - \gamma_{Aj}^r \gamma_{Bj+1}^r]. \quad (8)$$

Pictorially, this kind of hybridization can be represented as in Fig.1. Blue (red) circles represent B (A)-type MFs. The yellow ellipses denote effective strong coupling between nearest neighbor MFs. Were Eq.(8) the full Hamiltonian, the ℓ and r chains would dimerize with opposite phases. In addition, four unpaired MFs appear in Fig.1: two (the red/A ones) located at U and two (the blu/B

ones) at D.

To account for the extra interactions Γ and ut , following Ref. [25] we refermionize the Hamiltonian by including $H_U + H_D$ and by rearranging the MFs at the boundaries. Three effective Dirac Fermions, d_A, d_B, d_{end} are required, located at the U weak link, and three more ones, f_A, f_B, f_{end} , at the D boundary, according to[26]:

$$H_{eff} = \frac{i}{2\sqrt{2}} tu \left[f_{end} (f_B - f_A^\dagger) - h.c. \right] + t \left[d_A^\dagger d_B + h.c. \right] - \frac{\Gamma}{2} \left[\sin \frac{\varphi}{2} \left(2d_{end}^\dagger d_{end} - 1 \right) - i\sqrt{2} \cos \frac{\varphi}{2} \left(d_{end} (d_B + d_A^\dagger) - h.c. \right) + \sin \frac{\varphi}{2} \left(d_B d_A + d_A^\dagger d_B^\dagger + d_A d_A^\dagger - d_B d_B^\dagger \right) \right], \quad (9)$$

where

$$\varphi = \phi_{\ell 1} - \phi_{rN} = \frac{2e}{\hbar c} \oint \vec{A} \cdot d\vec{\ell}. \quad (10)$$

is the phase difference at the U weak link. The total energy only depends on the flux threading the ring, $\Phi = \oint \vec{A} \cdot d\vec{\ell}$, in units of ϕ_0 . This Bogolubov-de-Gennes (BdG) Hamiltonian H_{eff} changes sign under the operation Ξ of exchanging particles with holes and conserves the Fermionic parity $\mathcal{P} = (-1)^{\sum_i f_i^\dagger f_i + d_i^\dagger d_i}$. It can be shown that the low energy spectrum only depends on the first term in the second line, which involves the Dirac fermion $d_{end} = (\gamma_{A1}^\ell + i \gamma_{AN}^r)/2$, and on terms involving f_{end}, f_{end}^\dagger with $f_{end} = (\gamma_{B1}^r + i \gamma_{BN}^\ell)/2$, which can be obtained by perturbation theory from the first term of the first line. In addition, residual interactions, not included in H_{eff} , can account for finite size effects. In particular an extra coupling $z_\alpha \Gamma \propto e^{-N}$ ($\alpha = \ell, r$) arises from realistic long range interactions between the edge MFs at each chain, when the simple $t = |\Delta|[1]$ limitation is relaxed.

We are led to the minimal 4X4 Hamiltonian in the Majorana representation, just involving the four relevant MFs:

$$H_M = i\Gamma \begin{pmatrix} 0 & \sin \frac{\varphi}{2} & z_\ell & 0 \\ -\sin \frac{\varphi}{2} & 0 & 0 & z_r \\ -z_\ell & 0 & 0 & u' \\ 0 & -z_r & -u' & 0 \end{pmatrix}, \quad (11)$$

in the basis $[\gamma_{A1}^\ell, \gamma_{AN}^r, \gamma_{B1}^\ell, \gamma_{B1}^r]$, with $u' = ut/\Gamma$.

Ring cut at the bottom point : $u = 0$.

When the control parameter u is set to zero, the ring is cut at the bottom point D and the system is equivalent to a linear topological π junction with phase difference φ and open ends. In this case, if the finite size couplings z_α are neglected (see Fig. 2 left panel), there is a crossing at zero energy and zero flux due to the MFs at the U point, signalling a change of parity in the GS when the flux changes sign. Together with it, two dispersionless zero

energy modes appear, corresponding to the dangling MFs at the open ends. However, the system is expected to be unstable with respect to finite size interactions described by the z_α couplings. Indeed as soon as one turns z_α on, a gap opens and the zero energy MBS disappears (see Fig. 2 b).

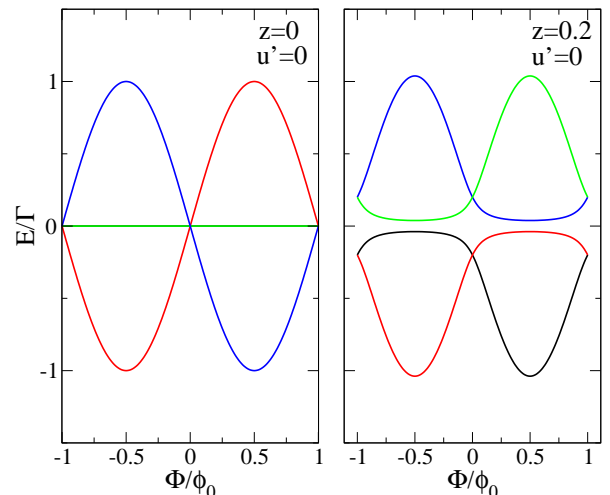


FIG. 2: (color online) Andreev Bound States as a function of the magnetic flux for an open ring ($u' = 0$). Left panel) Finite size corrections not included $z_l = z_r = 0$. Right panel) When finite size corrections are included $z_l = z_r = 0.2$ there is a splitting of the zero energy Andreev Bound State.

π -ring configuration: $u \neq 0$.

In the ring configuration ($u \neq 0$), the situation is quite different (see Fig. 3). The zero energy MBS is always present, no matter how strong the finite size effects z_α are. In the non-symmetric case ($z_\ell \neq z_r$), the location of the crossing occurs at non zero flux. With increasing of u' , the flux of the crossing point drifts towards $\varphi = 0$ (see Fig. 3 bottom panels). For the physically relevant case $u' \gg z_\ell, z_r$, just the crossing Andreev bound states survive at low energy and the dispersion turns out to

be approximately symmetric. The dispersion of the two crossing low lying energies tends to

$$E_{\pm} \sim \Gamma \sin\left(\frac{\varphi}{2}\right) \langle 2n_{end} - 1 \rangle_{\mathcal{P}} = \pm \Gamma \sin\left(\frac{\varphi}{2}\right). \quad (12)$$

With the labeling of the average $\langle \dots \rangle_{\mathcal{P}}$ we denote the fermionic parity of the GS. The minimum is for $\varphi \approx \pm\pi$ (i.e. flux $\pm\phi_0/2$), depending on the occupancy observable $n_{end} = d_{end}^{\dagger} d_{end}$ of the MBS located at the Josephson Junction.

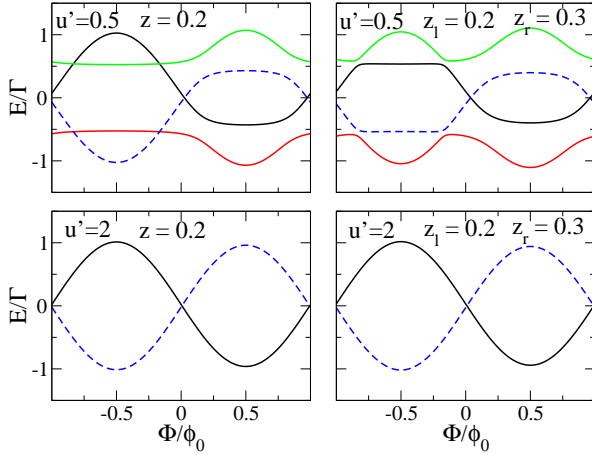


FIG. 3: (color online) Andreev Bound States as a function of the flux for the π ring. Left panels) No asymmetry $z = z_{\ell} = z_r$. Right panels) Asymmetrical case: $z_{\ell} \neq z_r$. An approximately symmetric spectrum is recovered for sizable u' , independently of the values of the asymmetry parameters z_{α} . In the closed ring geometry the zero energy Majorana Bound State is always present.

Model free energy and stationary conditions of the rf-SQUID.

We have shown that, in the topologically non trivial π -ring structure, an unpaired zero energy MBS exists and it is robust with respect to perturbations. This shows up as a crossing of the particle and hole excitation dispersions at flux close to zero. Our π -ring modelizes a topologically non trivial rf-SQUID device and we now argue that the MBS characterizes in a measurable way the stationary conditions of the device.

If the ring has a small diameter, so that its self-inductance L cannot be disregarded, the free energy is a function of the circulating current and of an external flux ϕ_{ext} which may be intentionally added. Its simplest form, arising from Eq.12 is:

$$F_{\mathcal{P}}(I, \phi_{ext}) = \frac{1}{2} L I^2 - \frac{\phi_0 I_c}{2\pi} \sin\left(\frac{\pi}{\phi_0}(\phi_{ext} + LI)\right) \langle 2n_{end} - 1 \rangle_{\mathcal{P}} \quad (13)$$

The free energy $F_{\mathcal{P}}(I, \phi_{ext} = 0)$ at zero external flux is plotted in Fig. 4a). The first and second minimum, belonging to the same \mathcal{P} , differ in phase by $\approx 2\pi$. Fig.4b

reports the change in shape of the free energy for one single \mathcal{P} , at different applied fluxes ϕ_{ext} .

The similarity with the conventional YBCO F π R is only superficial. At first sight Fig. 4b could report the free energy plot of a conventional F π R. By fine-tuning the external flux the two energy minima can be made degenerate. If \mathcal{P} is strictly conserved, this would be the end of the story and no difference would arise. However, in the topologically non trivial case, there is a corresponding set of curves belonging to the other \mathcal{P} . A switching between the two different minima e.g. at $\phi_{ext} = 0$ (see Fig. 4a) not only requires a flux quantum entering or exiting the ring but a simultaneous change of \mathcal{P} .

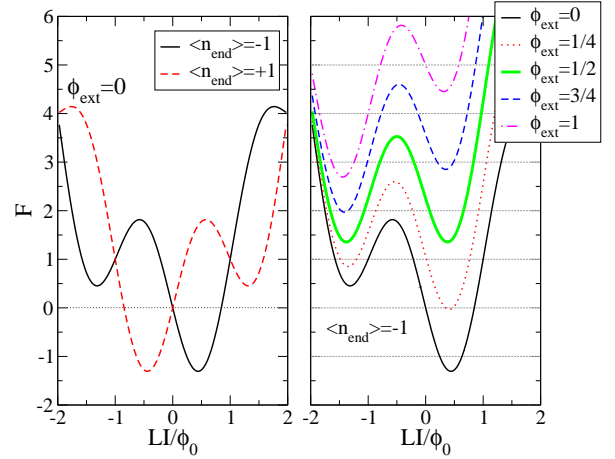


FIG. 4: (color online) a): free energy vs LI/ϕ_0 at zero external magnetic field for $\phi_{ext} = 0$ ($u =$ and $z_{\ell} = z_r =$). Full (dashed) line belong to the two different fermion parity \mathcal{P} . b): Corresponding free energy for different values of the external magnetic flux and one single parity. The curves are displaced in energy for clarity

A tool to fix the parity could be a side quantum point contact (QPC) controlling the charge tunneling. Addition of an electron on the ring would suddenly require the switching of the whole device between the two possible GSs, corresponding to a jump in the trapped spontaneous flux. By contrast, a conventional F π R is expected to be widely insensitive to the in-out tunneling of induced charges. Operating with a side gate on the QPC allows to distinguish a topological non trivial ring from a conventional one.

However, in real life, the job of fixing \mathcal{P} appears to be rather hard. The ring is not expected to be isolated: background impurities could provide charge noise, by releasing or capturing charges. For a system open to the environment, the energy spectrum of the isolated ring loses meaning and a description of the state of affairs in terms of the statistical density matrix $\hat{\rho}(t)$ is required. The latter accounts for the transitions, with absorption and emission of the energy between the two parities and with simultaneous switching of the flux. Under these

conditions, the expectation value of the observable corresponding to the flux, is likely to average to zero:

$$\lim_{t \rightarrow \infty} \langle \Phi \rangle = \text{Tr} \{ \hat{\rho} \Phi \} \sim 0 \quad (14)$$

Hence, we conclude that if we prepare the system in one of the two wells with initial flux $\sim \pm \phi_o/2$ and we leave the system to evolve freely by turning off the external flux, a measurement of the flux threading the ring after relaxation has taken place gives a null result. This is in striking contrast with a conventional tricrystal YBCO structure, which would not abandon the state supporting the spontaneous half flux quantum, and stays as a distinctive fingerprint of the presence of MFs.

We acknowledge enlightening discussions with P. Brouwer and A. Golubov. Financial support from FIRB 2012 project "HybridNanoDev" (Grant No.RBFR1236VV), FP7/2007-2013 (Grant N. 264098) - MAMA and MIUR PRIN 2009 project "Nanowire high critical temperature superconductor field-effect devices" are gratefully acknowledged.

-
- [1] A. Kitaev, Physics-Uspekhi **44**, 131 (2001).
 - [2] J. Alicea, Rep.Prog.Phys. **75**, 076501 (2012).
 - [3] J. Teo and C. Kane, Physical Review B **82**, 115120 (2010).
 - [4] R. M. Lutchyn, J. D. Sau, and S. Das Sarma, Physical Review Letters **105**, 077001 (2010).
 - [5] Y. Oreg, G. Refael, and F. von Oppen, Physical Review Letters **105**, 177002 (2010).
 - [6] M. Duckheim and P. W. Brouwer, Physical Review B **83**, 054513 (2011).
 - [7] H. Weng, G. Xu, H. Zhang, S.-C. Zhang, X. Dai, and Z. Fang, Physical Review B **84**, 060408 (2011).
 - [8] M. Kjærgaard, K. Wölms, and K. Flensberg, arxiv p. 1111.2129v1 (2011).
 - [9] J. Alicea, Physical Review B **81**, 125318 (2010).

- [10] L. Fu and Kane, Physical Review Letters **102**, 216403 (2009).
- [11] A. R. Akhmerov, J. Nilsson, and C. Beenakker, Physical Review Letters **216404**, 102 (2009).
- [12] Y. Tanaka, T. Yokoyama, and N. Nagaosa, Physical Review Letters **107002**, 103 (2009).
- [13] J. Linder, Y. Tanaka, A. Yokoyama, Sudbø, T., and N. Nagaosa, Physical Review Letters **067001**, 104 (2010).
- [14] A. Potter and P. Lee, Physical Review B **83**, 144522 (2011).
- [15] R. M. Lutchyn, T. D. Stanescu, and S. Das Sarma, Physical Review Letters **106**, 127001 (2011).
- [16] P. W. Brouwer, M. Duckheim, F. Romito, and F. von Oppen, Physical Review Letters **107**, 196804 (2011).
- [17] V. Mourik, K. Zuo, S. Frolov, S. Plissard, E. Bakkers, and L. Kouwenhoven, Science **336**, 1003 (2012).
- [18] M. T. Deng, C. L. Yu, G. Y. Huang, M. Larsson, P. Caroff, and H. Q. Xu, Nano Letters **xx**, xxx (2012).
- [19] A. Das, Y. Ronen, Y. Most, Y. Oreg, M. Heiblum, and H. Shtrikman, Nature Physics **8**, 887 (2012).
- [20] E. J. H. Lee, X. Jiang, R. Aguado, G. Katsaros, C. M. Lieber, and S. De Franceschi, Phys. Rev. Lett. **109**, 186802 (2012).
- [21] C. C. Tsuei, J. R. Kirtley, C. C. Chi, L. S. Yu-Jahnes, A. Gupta, T. Shaw, J. Z. Sun, and M. B. Ketchen, Phys. Rev. Lett. **73**, 593 (1994).
- [22] C. C. Tsuei and J. R. Kirtley, Review of Modern Physics **72**, 969 (2000).
- [23] M. Sigrist and T. M. Rice, Rev. Mod. Phys. **67**, 503 (1995).
- [24] P. Lucignano, A. Mezzacapo, F. Tafuri, and A. Tagliacozzo, Phys. Rev. B **86**, 144513 (2012).
- [25] J. Alicea, Y. Oreg, G. Rafael, F. von Oppen, and M. Fisher, Nature Physics **7**, 412 (2011).
- [26] Here the definition of the relevant fermions: $d_{end} = \frac{1}{2}(\gamma_{LA1} + i\gamma_{RAN})$, $d_1 = \frac{1}{2}(\gamma_{LA2} + i\gamma_{LB1})$, $f_{N-1} = \frac{1}{2}(\gamma_{RBN} + i\gamma_{RAN-1})$, $d_A = \frac{1}{\sqrt{2}}(d_1 + f_{N-1})$, $d_B = \frac{1}{\sqrt{2}}(d_1 - f_{N-1})$, $f_{end} = (\gamma_{RB1} + i\gamma_{LBN})/2$, $d_{N-1} = \frac{1}{2}(\gamma_{LAN} + i\gamma_{LBN-1})$, $f_1 = \frac{1}{2}(\gamma_{RB1} + i\gamma_{RA2})$, $f_A = (f_1 + / - d_{N-1})/\sqrt{2}$, $f_B = (f_1 + / - d_{N-1})/\sqrt{2}$.